Functionalized Diblock Copolymer of Poly(ε-caprolactone) and Polyphosphoester Bearing Hydroxyl Pendant Groups: Synthesis, Characterization, and Self-Assembly

Wen-Jing Song,[†] Jin-Zhi Du,[‡] Nan-Jun Liu,[‡] Shuang Dou,[†] Jing Cheng,[‡] and Jun Wang*[,†]

Hefei National Laboratory for Physical Sciences at Microscale and School of Life Sciences and Department of Polymer Science and Engineering, University of Science and Technology of China, Hefei, Anhui 230027, P.R. China

Received May 8, 2008; Revised Manuscript Received July 18, 2008

ABSTRACT: Novel diblock copolymers of poly(ε-caprolactone) and polyphosphoester bearing functional hydroxyl pendant groups, denoted as PCL-*b*-PHEP, were synthesized through ring-opening polymerization of functionalized cyclic phosphoester monomer using hydroxyl end-capped poly(ε-caprolactone) and $Sn(Oct)_2$ as macroinitiator and catalyst, respectively. The chemical structure was proved by ^1H, ^{13}C, and ^{31}P NMR, gel permeation chromatography (GPC), and Fourier transform infrared spectroscopy (FT-IR) analyses. These amphiphilic functionalized block copolymers could self-assemble into micellar or vesicular aggregates in aqueous solution, depending on the composition, which was demonstrated by transmission electron microscopy and confocal laser scanning microscope observations. The critical aggregation concentrations (CAC) of PCL-*b*-PHEP were also dependent on the composition, measured by the fluorescence probe technique. MTT assay for cytotoxicity of PCL-*b*-PHEP suggested these polymeric nanoparticles were biocompatible. Combining the advantages of poly(ε-caprolactone) and polyphosphoester with functional hydroxyl pendant groups for further biological modification, such amphiphilic block copolymers could potentially provide novel opportunities for design of drug delivery system and therapeutic application.

Introduction

Aliphatic polyesters, such as poly(ε-caprolactone) (PCL), polylactide (PLA), polyglycolide (PGA), and their copolymers, have been widely used in polymer-based biomaterials due to their demonstrated biodegradability and biocompatibility.[1−3] Medical applications of aliphatic polyesters typically include drug delivery vehicles, suture, implants, and tissue engineering scaffolds.[4−6] However, their applications are limited in scope due to their hydrophobic, semicrystalline properties, and the absence of functionality on the polymer backbone.[7]

In contrast to the above polyesters, polyphosphoester (PPE), which has currently been studied extensively in drug, gene delivery, and tissue engineering,[8−10] possesses adjustable physical and chemical properties. PPEs are a series of hydrophilic biomaterials and, more importantly, have the unique advantage on functionalization ability due to the pentavalent nature of the phosphorus atom. Therefore, novel functionalized biodegradable PPEs bearing reactive pendant groups such as hydroxyl, carboxyl, amino groups, and so forth become available. The combination of water solubility and reactive pendant functional groups made PPEs possible new functional biomaterials to be applied in the construction of novel controlled drug delivery systems or other related biomedical applications.

In general, pendant functionalization of polymers can be achieved by postpolymerization modification or polymerization of functionalized monomers.[11,12] In the case of postpolymerization modification, the conditions chosen must not induce degradation or undesired cross-linking. On the other hand, when polymerizing functionalized monomers, the functionality must be chemically compatible with the polymerization conditions or preprotected before polymerization. In the numbered reported examples of PPE bearing functional pendant groups, Wang et al. utilized the postpolymerization modification method to obtain a series of cationic PPE with different side charge groups, which served as effective, nontoxic, and biodegradable gene carriers.[9] Huang et al. used the same method to synthesize a water-soluble, nonionic PPE with hydroxyl side group, which allows the fine-tuning of the physicochemical properties to enhance gene expression in muscle,[13] while Du et al. used the latter method to synthesize functional triblock copolymers based on poly(ethylene glycol) and PPE with pendant vinyl groups by direct ring-opening polymerization of cyclic phosphoester monomer containing double bonds.[14] It is worth noting that all the PPEs above-mentioned are water-soluble but not amphiphilic. In fact, to our best knowledge, amphiphilic graft polymers of PPEs have been studied for their self-assemblies,[15] but no amphiphilic block copolymers containing functional PPE have been reported up to now.

It is well-known that amphiphilic copolymers will self-assemble spontaneously into polymeric aggregates including micellar and vesicular conformations.[16] Because of enhanced permeation and retention (EPR) effect of nanoparticles in tumor tissues, the nanosized polymeric aggregates have received much attention as useful drug delivery carriers for various anticancer drugs.[17,18] However, such passive targeting strategy is not sufficient in practical applications. Many efforts have been made to impart the vehicles with active targeting ability,[19,20] which in reverse calls for functionality of the polymer materials. Thus, design and synthesis of amphiphilic and functionalized polymers are necessary and urgent.

In the present work, we adopted the polymerization of preprotected functional monomer method to obtain hydroxyl-functionalized amphiphilic polymers. By this method, the phosphoester monomer 2-(2,2-dimethyl-1,3-dioxolan-4-yl-methoxy)-2-oxo-1,3,2-dioxaphospholane (GEP) as shown in Scheme 1, whose hydroxyl pendant groups were protected by the 1,3-

* To whom correspondence should be addressed: Fax +86 551 360 0402; e-mail jwang699@ustc.edu.cn.
[†] Hefei National Laboratory for Physical Sciences at Microscale and School of Life Sciences.
[‡] Department of Polymer Science and Engineering.

10.1021/ma801043m CCC: $40.75
Published on Web 09/03/2008

Scheme 1. Synthesis Routes of Phosphoester Monomer GEP and Functionalized Diblock Copolymer of Poly(ε-caprolactone) and Polyphosphoester PCL-*b*-PHEP

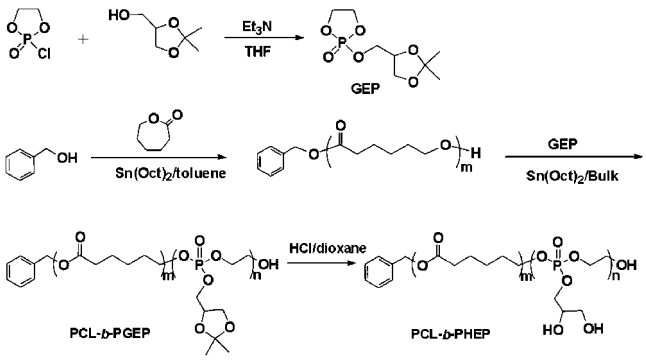

dioxolane ring, was polymerized with the initiation of hydroxyl end-capped poly(ε-caprolactone). After deprotection under mild conditions, the amphiphilic hydroxyl-functionalized block copolymers PCL-*b*-PHEP were obtained. The preparation, characterization, and self-assembly behavior of the copolymers were described.

Experimental Section

Materials. 2-Chloro-2-oxo-1,3,2-dioxaphospholane (COP) was synthesized by a method described previously and distilled under reduced pressure before use.[21,22] 2,2-Dimethyl-4-hydroxymethyl-1,3-dioxolane was synthesized according to a method reported elsewhere[23] and distilled under reduced pressure before use. Toluene was refluxed over sodium and distilled under nitrogen prior to use. ε-Caprolactone (CL) (Acros Organics, 99%) was dried over calcium hydride for 48 h at room temperature, followed by distillation under reduced pressure just before use. Benzyl alcohol (BnOH, Sinopharm Chemical Reagent Co., Ltd., China) was analytical grade and distilled before use. Triethylamine (Sinopharm Chemical Reagent Co., Ltd., China) was refluxed with phthalic anhydride, potassium hydroxide, and calcium hydride in turn and distilled before use. Tetrahydrofuran (Sinopharm Chemical Reagent Co., Ltd., China) was refluxed over potassium−sodium alloy under a N_2 atmosphere and distilled. Stannous octoate ($Sn(Oct)_2$, Sinopharm Chemical Reagent Co., Ltd., China) was purified according to a method described in the literature.[24] Fluorophore dye PKH26 and 3-(4,5-dimethylthiazol-2-yl)-2,5-diphenyltetrazolium bromide (MTT) were obtained from Sigma Chemical Co. Pyrene (Acros Organics) and other solvents were used as received.

Synthesis of Monomer GEP. To a 250 mL flame-dried flask equipped with a dropping funnel and a stirring bar was added a solution of 2,2-dimethyl-4-hydroxymethyl-1,3-dioxolane (13.22 g, 0.1 mol) and anhydrous triethylamine (10.12 g, 0.1 mol) in 120 mL of fresh dried THF. After cooling at −5 °C for 30 min, 2-chloro-2-oxo-1,3,2-dioxaphospholane (COP) (14.25 g, 0.1 mol) in 30 mL of anhydrous THF was added dropwise at −5 °C to the stirred solution over a period of half an hour. The mixture was maintained at −5 °C overnight. The precipitate, triethylammonium chloride, was filtered off using a Schlenk funnel. The filtrate was concentrated under vacuum, and the residue was purified by recrystallization in 200 mL of anhydrous THF/diethyl ether (1:10, v/v) twice to obtain a white product with a yield of 63%. ^1H, ^{13}C, and ^{31}P NMR spectra supported the structure shown in Scheme 1.

Synthesis of Poly(ε-caprolactone) Macroinitiator. Poly(ε-caprolactone) (PCL) was synthesized through ring-opening polymerization of CL in anhydrous toluene using benzyl alcohol as an initiator and $Sn(Oct)_2$ as the catalyst. Typically, CL (28.5 g, 0.25 mol), benzyl alcohol (0.45 g, 4.2 mmol), $Sn(Oct)_2$ (0.42 g, 1 mmol), and anhydrous toluene (125 mL) were added into a fresh flamed and nitrogen-purged round-bottomed flask in a glovebox with H_2O content less than 0.1 ppm. The mixture was maintained at 80 °C for 12 h. Toluene was evaporated under reduced pressure, and the mixture was precipitated into cold diethyl ether twice. The precipitate was dried under vacuum to a constant weight at room temperature with a yield of 92.7%.

Synthesis of Block Copolymer PCL-*b*-PGEP. Block copolymerization was carried out in bulk by ring-opening polymerization of GEP using PCL macroinitiator and stannous octoate as the catalyst. Before polymerization, macroinitiator was purified twice by azeodistillation of anhydrous toluene and dried under vacuum. Typically, in a glovebox with water content lower than 0.1 ppm, PCL macroinitiator (0.14 mmol) and GEP (5.5 mmol) were consecutively added into a 25 mL freshly flamed and nitrogen-purged flask. After stirring at 90 °C for 10 min, $Sn(Oct)_2$ (0.03 mmol) was added. The reaction was carried out for an additional 3 h. The polymer was dissolved in chloroform and precipitated into methanol/ether (1:10, v/v) twice. The copolymer was obtained and dried under vacuum at room temperature with a yield of 62.5%.

Synthesis of Block Copolymer PCL-*b*-PHEP. In a typical procedure, aqueous hydrochloric acid (1 mol L^{-1}, 10 mL) was added dropwise to the solution of PCL-*b*-PGEP block copolymer (0.36 g) in 30 mL of 1,4-dioxane. The solution was stirred at room temperature for 3 h. The solution was concentrated and then poured into diethyl ether to precipitate the polymer. The deprotected polymer PCL-*b*-PHEP was dried under vacuum to yield white product (90% yield).

Characterization. Structural characterizations were performed via ^1H, ^{13}C, and ^{31}P NMR spectroscopies, which were recorded on a Bruker AV300 NMR spectrometer (300 MHz) at room temperature with $CDCl_3$ or d_6-DMSO as solvent and TMS as internal reference. Phosphoric acid (85%) was used as an external reference for ^{31}P NMR analyses. FT-IR spectra were measured on a Bruker Vector 22 Fourier transform infrared spectrometer at wave numbers 400−4000 cm^{-1} with a resolution of 2 cm^{-1} using the KBr disk method.

Number- and weight-average molecular weights (M_n and M_w) and molecular weight distributions (polydispersity index, PDI = M_w/M_n) of polymers were determined by gel permeation chromatography (GPC) measurements on a Waters GPC system, which was equipped with a Waters 1515 HPLC solvent pump, a Waters 2414 refractive index detector, and three Waters Styragel high-resolution columns (HR4, HR2, and HR1, effective molecular weight range 5000−500 000, 500−20 000, and 100−5000, respectively) at 40 °C. Chloroform (HPLC grade, J.T. Baker, stabilized with 0.75% ethanol) was used as eluent and delivered at a flow rate of 1.0 mL min^{-1}. Monodispersed polystyrene standards with a molecular weight range 1310−5.51 × 10^4 were used to generate the calibration curve. It was noteworthy that the actual molecular weights of aliphatic polyesters (e.g., PCL) were ∼0.56 times lower than the average molecular weights calculated from the polystyrene calibration curve, which was systematically studied by Biela et al. and Save et al. elsewhere.[25,26]

Preparation of PCL-*b*-PHEP Aggregates. The aggregates of PCL-*b*-PHEP were either prepared by a dialysis method or film rehydration method. In a dialysis process, 10 mg of block copolymer was dissolved in 1 mL of *N, N*-dimethylformamide (DMF). Under moderate stirring the predetermined volume (5 mL) of ultrapurified water (Millipore, 18.2 MΩ) was added. The mixture was left stirring for an additional 3 h. DMF was then removed by dialysis against water for at least 24 h to obtain the aggregates.

In film rehydration process, a certain amount of PCL-*b*-PHEP was dissolved in $CHCl_3$ at a total polymer concentration of 10 g L^{-1}. Then the polymer solution was evaporated to dryness in a round-bottomed flask using a rotary evaporator at room temperature to obtain a thin film on the inner surface of the flask, which was further dried under vacuum overnight. The film was resuspended in ultra purified water at a concentration of 2 g L^{-1}. The suspension was sonicated using a bath sonicator for 2−5 h discontinuously at room temperature to form homogenized nanoparticles after the mixture was incubated in a water bath at 50 °C for 30 min with occasional shaking. Then, an aliquot PKH26 stock solution was added to the suspension and incubated for 2 h at 4 °C, followed by subjecting to dialysis to remove excess dye.

Particle Size and Zeta Potential Measurements. The size and size distribution of micelles in aqueous solution were measured by dynamic light scattering (DLS) carried out on a Malvern Zetasizer Nano ZS90 with a He−Ne laser (633 nm) and 90° collecting optics. All samples were prepared in aqueous solution at a concentration of 0.2 g L^{-1} and filtered through Millipore 0.45 μm filter prior to measurements. All measurements were carried out at 25 °C, and data were analyzed by Malvern Dispersion Technology Software 4.20. The zeta potential measurements were performed using an aqueous dip cell in automatic mode using Malvern Zetasizer Nano ZS90.

Transmission Electron Microscopy (TEM). The morphology examination of the copolymer micelles prepared by dialysis method was performed on a Hitachi model H-800 transmission electron microscope with an accelerating voltage of 200 kV. A drop of the solution (0.5−1 g L^{-1}) was then cast onto a 200-mesh carbon-coated copper grid. The samples were finally dried at room temperature prior to measurements.

Confocal Laser Scanning Microscopy (CLSM). The PCL-*b*-PHEP aggregates were prepared by film rehydration method. The slides were mounted and observed with a Zeiss LSM510 laser confocal scanning microscope imaging system (Germany) with an upright confocal microscope and a 40× objective. The data were analyzed by LSM 5 Image Examiner software.

Critical Aggregation Concentration (CAC) Determination. To estimate the CAC of the aggregates, pyrene was used as the fluorescence probe. A predetermined amount of pyrene in acetone was added into a series of ampules, and the acetone was then removed first by gently flowing N_2 and then by vacuum. A predetermined volume of copolymer solutions and ultrapurified water were added into the ampules consecutively to get solutions of different micelle concentrations ranging from 1.0×10^{-5} to 1 g L^{-1}, while the concentration of pyrene in each flask was fixed at 6.0×10^{-7} mol L^{-1}, slightly lower than the saturation solubility of pyrene in water. Fluorescence spectra were recorded on a Shimadzu RF-5301PC spectrofluorophotometer at 390 nm emission wavelength and 3 nm slit width.

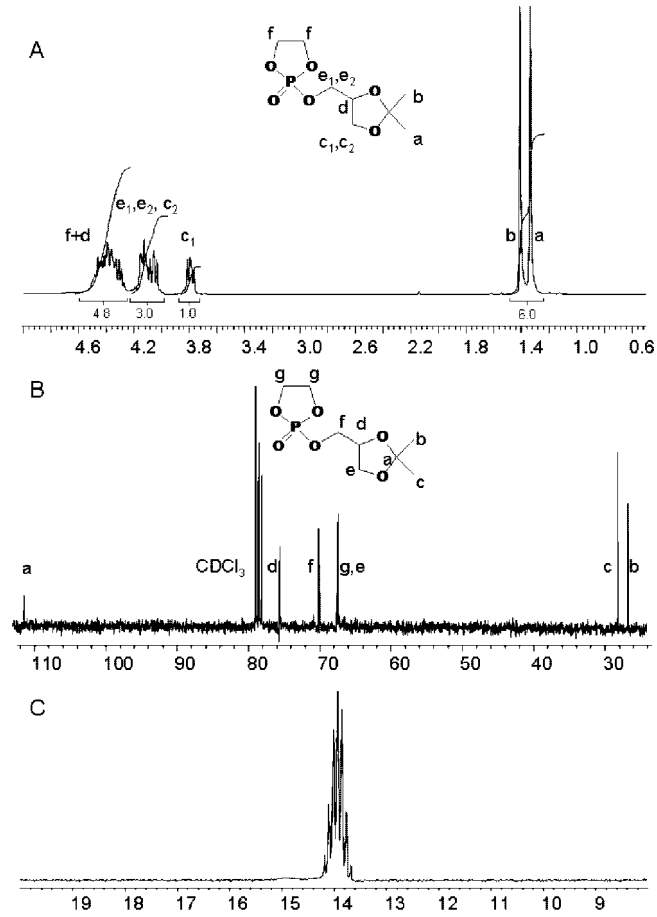

Figure 1. NMR spectra of monomer GEP (in $CDCl_3$, ppm). (A) ^1H NMR, (B) ^{13}C NMR, (C) ^{31}P NMR.

Results and Discussion

Synthesis and Characterization of Block Copolymer PCL-*b*-PGEP. Synthesis of polyphosphoesters was pioneered by Penczek and his colleagues at the end of the 1970s. They have studied extensively the synthesis and elucidated many of the mechanisms of different routes, including anionic and cationic ring-opening polymerizations,[27,28] polycondensation,[29,30] and polyaddition.[31] On the basis of their studies, we have previously demonstrated that polyphosphoesters can be synthesized by ring-opening polymerization (ROP) of five-membered cyclic phosphoester monomer (i.e., 2-ethoxy-2-oxo-1,3,2-dioxaphospholane, EEP) using the alcohol and stannous octoate co-initiation system.[32] It has been reported that the yielded polyphosphoester has defined molecular structure. Further kinetic studies demonstrate that the ROP is a first-order reaction with respect to phosphoester monomer, suggesting a coordination−insertion polymerization mechanism.[33] Subsequently, we also successfully synthesized the triblock copolymer of poly(ethylethylene phosphate) with PCL (PEEP-*b*-PCL-*b*-PEEP) using a similar method, while the dihydroxyl-terminated PCL and stannous octoate co-initiation system was used.[8] In this study, to synthesize functionalized diblock copolymer of PCL and polyphosphoester bearing hydroxyl pendant groups, we took the advantage of such polymerization method, while stannous octoate was used as the catalyst. The macroinitiator, which is hydroxyl-terminated PCL (PCL-OH), was synthesized by polymerization of CL and further utilized for polymerization of functionalized phosphoester monomer GEP, as shown in Scheme 1.

To synthesize PCL-*b*-PGEP block copolymer, we first prepared the monomer GEP. The synthesis procedure, shown in Scheme 1, was via the reaction of 2-chloro-2-oxo-1,3,2-dioxaphospholane (COP) with 2,2-dimethyl-4-hydroxymethyl-1,3-dioxolane, which was similar to the synthesis of EEP.[34] GEP was purified by recrystallization from anhydrous THF/diethyl ether twice. ^1H, ^{13}C, and ^{31}P NMR spectra are shown in Figure 1, and all the resonances were assigned as illustrated.

The macroinitiator (PCL-OH) was obtained by polymerization of CL in toluene using benzyl alcohol as the initiator and $Sn(Oct)_2$ as the catalyst, which has actually been the most often used for ROP of lactone and lactide due to its high catalytic activity as well as US FDA approval as a food additive.[35] The average degree of polymerization (DP) of PCL-OH was calculated from its ^1H NMR spectrum (typically, shown in Figure 2A) based on the integration ratio of triplet at 4.07 and 3.67 ppm, assigned to methylene protons *f* and *g*, respectively. All macroinitiators showed symmetrical and monomodal molecular weight distributions with narrow polydispersity indexes (PDI) less than 1.21. The properties of PCL-OH used in this study are summarized in Table 1. From Table 1, it was also clearly seen that the M_n(GPC) incompletely matched to M_n(NMR), which was attributed to the fact that monodispersed polystyrenes were used as standards for GPC calibration. Such a phenomenon was also observed by many other groups in GPC analysis of PCL and PLA.[25,26,36]

Subsequently, we utilized the PCL-OH macroinitiator and GEP monomer for the preparation of PCL-*b*-PGEP diblock copolymer. The polymerization was initially carried out in THF at 40 °C as described previously for EEP polymerization.[32] However, conversion of GEP was rather low according to GPC analyses (results not shown), indicating that the polymerization of GEP in THF was obstructed. We speculated that the major

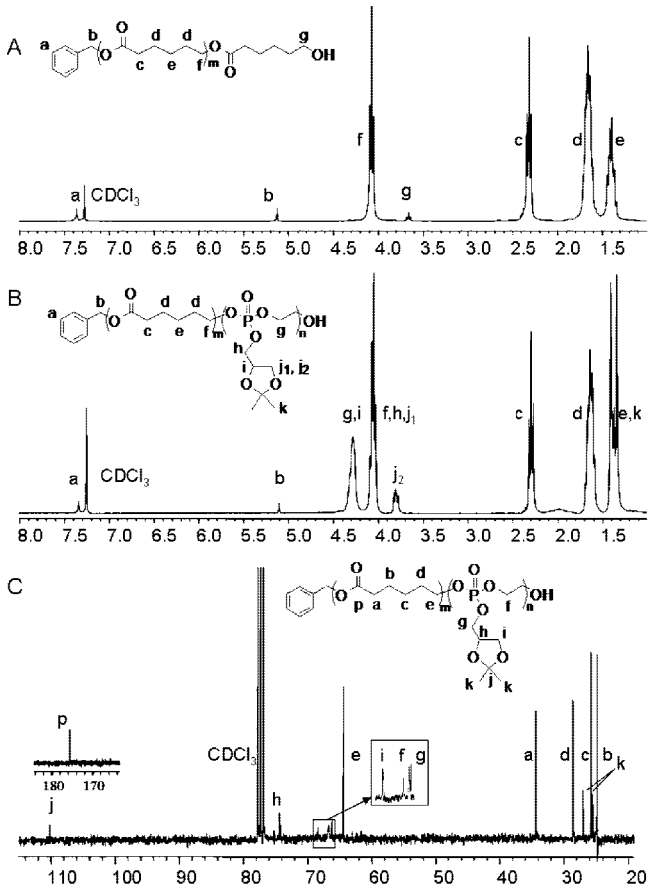

Figure 2. ^{1}H NMR spectra of PCL_{30} (A) and PCL_{30}-*b*-$PGEP_{13}$ (B) and ^{13}C NMR spectrum of PCL_{30}-*b*-$PGEP_{13}$ (C) in $CDCl_3$ (ppm).

Table 1. Characterization of PCL-OH Macroinitiators

sample	feed ratio $[CL]_0/[BnOH]_0$	DP of PCL[a]	M_n[a]	M_n[b]	PDI[b]
PCL_{30}	35:1	30	3530	3100	1.10
PCL_{50}	60:1	50	5810	5430	1.11
PCL_{75}	80:1	75	8660	10570	1.21
PCL_{100}	120:1	100	11510	16720	1.19

[a] Determined by ^{1}H NMR. [b] GPC values corrected with the coefficient 0.56 (see Experimental Section).

reason is the influence of the GEP starting concentration on the equilibrium position. Earlier work of Penczek et al. has demonstrated that at higher starting concentration (bulk) the proportion of monomer that does polymerize was higher.[27] In addition, the monomer steric hindrance may also affect the polymerization. In fact, we have observed that the rate of polymerization of five-membered phosphoester monomers (2-alkoxyl-2-oxo-1,3,2-dioxaphospholane, which are analogues of EEP) was significantly affected by the alkoxyl groups when alcohol and $Sn(Oct)_2$ co-initiation was applied in THF. Variation of alkoxyl groups from ethoxyl to *n*-propoxyl and *n*-butoxyl resulted in decreased polymerization rates and increased Arrhenius activation energies for polymerization in the sequence of ethoxyl, *n*-propoxyl, *n*-butoxyl substituted monomers. Especially, the isopropoxyl-substituted monomer 2-isopropoxyl-2-oxo-1,3,2-dioxaphospholane could not be polymerized under the same conditions.

Therefore, we attempted polymerization of GEP in bulk at 90 °C using the PCL-OH and $Sn(Oct)_2$ co-initiation system and found that the polymerization went on, indicated by the increased viscosity. As shown in Figure 3, the GPC chromatograms of PCL-OH macroinitiator and obtained PCL-*b*-PGEP block copolymer were compared, and the unimodal peak of

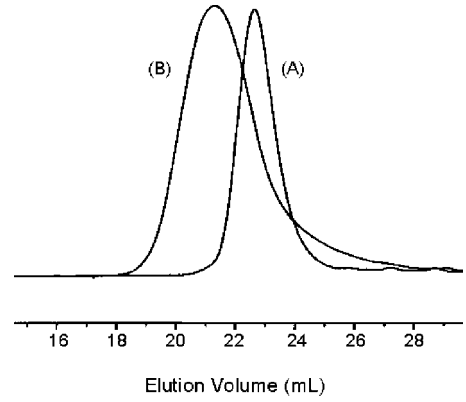

Figure 3. GPC chromatograms of (A) PCL_{30} and (B) PCL_{30}-*b*-$PGEP_{25}$.

Table 2. Composition and Molecular Weight of Block Copolymer PCL-*b*-PGEP

sample	feed ratio of $[GEP]_0/[PCL\text{-}OH]_0$	conversion of GEP (%)[a]	M_n[a]	M_n[b]	PDI[b]
PCL_{30}-*b*-$PGEP_{13}$	20:1	65	6620	6840	1.45
PCL_{30}-*b*-$PGEP_{25}$	40:1	62.5	9480	8950	1.30
PCL_{50}-*b*-$PGEP_{10}$	15:1	66.7	8180	10150	1.38
PCL_{50}-*b*-$PGEP_{15}$	20:1	75	9380	10570	1.40
PCL_{75}-*b*-$PGEP_{15}$	20:1	75	12220	18260	1.42
PCL_{100}-*b*-$PGEP_{18}$	33:1	54	15780	22840	1.30

[a] Determined by ^{1}H NMR. [b] GPC values corrected with the coefficient 0.56 (see Experimental Section).

PCL-*b*-PGEP with decreased retention time demonstrated the successful polymerization of GEP and the formation of copolymer in such conditions. The conversion of GEP was in the range of 54%−75% in our experiments (summarized in Table 2). No peaks of PGEP homopolymer and polymer of high molecular weight were observed in the GPC chromatograms. Meanwhile, the number-average molecular weight (M_n) of PCL-*b*-PGEP was linearly dependent on the GEP conversion (see Supporting Information, Figure S1), revealing that scarce inter- or intramolecular transesterification side reactions occurred during the polymerization in bulk, which was actually ensured by their molecular weight distributions (from 1.3 to 1.45) given in Table 2. Moreover, there was a slight tail on the GPC chromatogram, which may be due to the interaction of polymer with the column. In addition, it should be noted that the M_n values obtained from ^{1}H NMR and GPC were not coincided mutually, which may be due to the same reason mentioned in PCL analysis.

Figures 2A, B show a comparison of ^{1}H NMR spectra of PCL_{30} and a typical diblock copolymer PCL_{30}-*b*-$PGEP_{13}$. It was found that all signals assigned to protons of PCL block (except the terminal methylene protons directly linked to the hydroxyl group) in Figure 2A were all present in the spectrum of block copolymer PCL_{30}-*b*-$PGEP_{13}$. Among those newly appearing signals in Figure 2B, resonances at 1.37 and 1.41 ppm were assigned to protons of the dimethyl group ($-C(CH_3)_2$) of the acetal protecting groups. In addition, resonances at 4.20−4.40 ppm were the characteristic signals of methylene protons (g) of the phosphoester backbone and the methine proton (i) of 1,3-dioxolane ring. The degree of polymerization of PGEP block, *n*, was calculated from the ratio between the peak integration of methylene protons of PCL block (c) and that of methyl protons of PGEP blocks (j_2).

The structure of copolymer was also confirmed by the ^{13}C NMR spectrum. All the signals were assigned as shown in Figure 2C. In particular, the characteristic signals of the dimethyl carbons (k) and the methine carbon (j) of the 1,3-dioxolane ring were clearly observed, which was in good agreement with the ^{1}H NMR spectrum, indicating the successful polymerization of

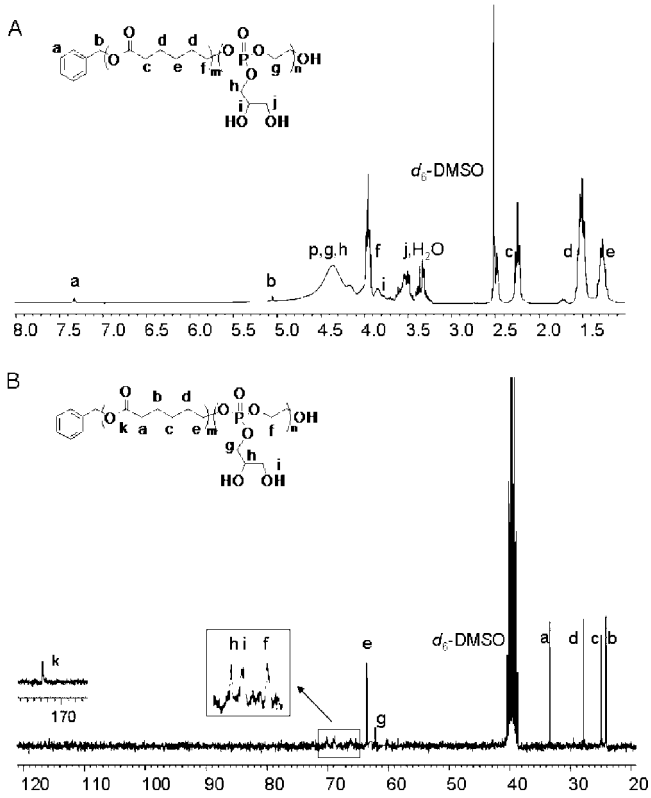

Figure 4. ^{1}H NMR (A) and ^{13}C NMR (B) spectra of PCL_{30}-*b*-$PHEP_{13}$ in d_6-DMSO (ppm).

GEP. In addition, the ^{31}P NMR spectrum (see Supporting Information, Figure S2A) of block copolymer gave a strong resonance at −4.50 ppm, assigned to the phosphorus atoms in polyphosphoester block.

Synthesis and Characterization of Block Copolymer PCL-*b*-PHEP. The 1,3-dioxolane ring in PCL-*b*-PGEP was readily cleaved to regenerate the diol functional groups by treating the copolymers for 3 h with 1 mol L^{-1} HCl in 1,4-dioxane at room temperature. In a typical ^{1}H NMR spectra of PCL_{30}-*b*-$PHEP_{13}$ (Figure 4A), the methyl proton signals of the 1,3-dioxolane ring at 1.37 and 1.44 ppm ($C(CH_3)_2$) thoroughly disappeared after deprotection. Likewise, in the ^{13}C NMR spectrum of PCL_{30}-*b*-$PHEP_{13}$ (Figure 4B), the methine carbon signal at 110.28 ppm (p) and the dimethyl carbons at 25.64 and 27.14 ppm (k) of the 1,3-dioxolane ring also disappeared, demonstrating the successful deprotection of the copolymer. It should be mentioned that peak of the carbonyl carbon in ^{13}C NMR spectrum after deprotection was still a single one, indicating no obvious side reaction occurred. Other carbon signals were assigned in the figure as well, confirming the intact structure of PCL-*b*-PHEP further. This was also solidated in by the ^{31}P NMR as shown in the Supporting Information, Figure S2B.

Besides, the FT-IR spectra also confirmed the successful deprotection. Figure 5 shows the comparison between FT-IR spectra of representative PCL-*b*-PGEP and PCL-*b*-PHEP. The deformation bands due to the geminal methyl group of the 1,3-dioxolane ring ($-C(CH_3)_2$) at 1369−1382 cm^{-1} almost disappeared after deprotection. Accordingly, the methyl ($-CH_3$) asymmetrical stretching band at 2986 cm^{-1} disappeared. Also, the disappearance of the peak at 838 cm^{-1} coming from the acetonide ring was in agreement with the removal of the protecting group.[37] On the other hand, absorbances at 1730 and 1045 cm^{-1} were characteristic absorptions of the C═O stretching and C−O stretching due to the presence of PCL block, while

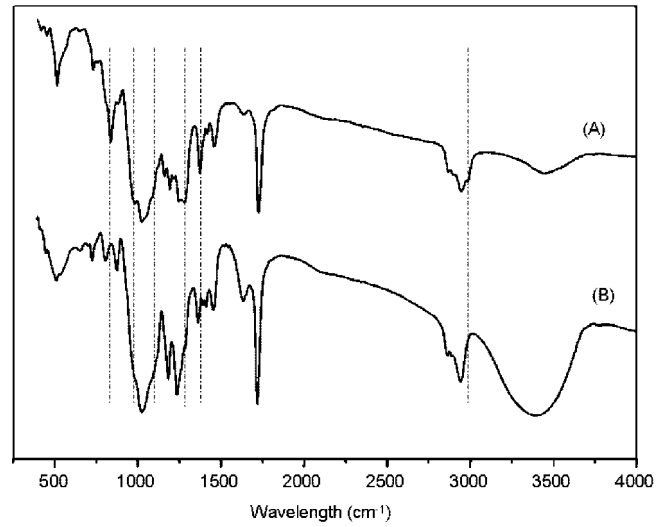

Figure 5. FT-IR spectra of (A) PCL_{30}-*b*-$PGEP_{13}$ and (B) PCL_{30}-*b*-$PHEP_{13}$.

absorptions of asymmetrical and symmetrical P═O stretchings occurred at 1280 and 1160 cm^{-1}, respectively, while P−O−C stretching appeared at 980 cm^{-1}, which demonstrated the PHEP block was still present after the deprotection reaction. Therefore, it is concluded that the ester group remained intact during the hydrolysis of the acetonide ring, consistent with the NMR analyses.

Self-Assembly of PCL-*b*-PHEP Copolymers. Amphiphilic block copolymers with hydrophilic and hydrophobic segments have been found to self-assemble spontaneously into polymeric aggregates in selective solvents. The laboratory preparation of polymeric aggregates is usually carried out in two steps, i.e., dissolving in a common solvent of both hydrophilic and hydrophobic segments and then aggregating upon replacement of the common solvent with a selective solvent. Usually, the common solvent is an organic solvent, and the selective solvent is water.[38]

PCL-*b*-PHEP copolymers consisted of hydrophobic PCL segments and hydrophilic PHEP segments. In this study, we used DMF as the common solvent for both of PCL and PHEP components. By adding water to copolymer solution in DMF under moderate stirring, following dialysis against water to remove organic solvent, we obtained self-assembled aggregates of PCL-*b*-PHEP copolymers.

As demonstrated by dynamic light scattering (DLS) measurements (Figure 6), all of copolymers formed aggregates with diameters from ∼70 to 120 nm, showing unimodal size distributions with PDI ∼ 0.1. Detailed information is summarized in Table 3. It was noted that with the increase of PCL length average diameter of the aggregates increased as well, indicating that a longer PCL block may enhance its assembly and lead to a larger dimension. Aggregates were found negatively charged, with an average zeta potential value of around −35 mV, which reveals a high electric charge on the surface of aggregates, and it may cause strong repellent forces among particles to prevent aggregation.[8]

The successful formation of aggregates by the dialysis method was further confirmed by TEM measurements. Parts A and B of Figure 7 show the typical TEM micrographs of aggregates of PCL_{30}-*b*-$PHEP_{13}$ and PCL_{50}-*b*-$PHEP_{15}$, respectively. It can be seen that aggregates of PCL_{30}-*b*-$PHEP_{13}$ took the spherical micellar morphology, while aggregates of PCL_{50}-*b*-$PHEP_{15}$ were likely in vesicular conformation with ca. 80 nm in diameter that were slightly larger than that observed by DLS measurements.

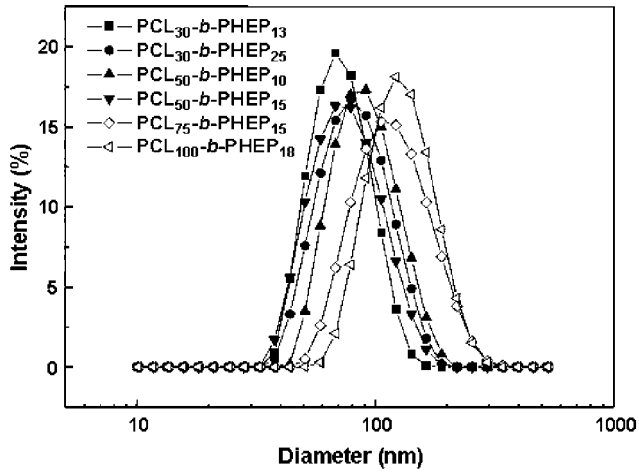

Figure 6. Particle size distribution of aggregates of PCL-*b*-PHEP copolymers.

Table 3. Properties of the Polymeric Aggregates

sample	CAC (g L^{-1})	diameter (nm)	PDI	zeta potential (mV)
PCL_{30}-*b*-$PHEP_{13}$	2.5×10^{-3}	68.8 ± 0.54	0.111 ± 0.021	−35.6
PCL_{30}-*b*-$PHEP_{25}$	4.6×10^{-3}	77.4 ± 0.63	0.088 ± 0.005	−35.7
PCL_{50}-*b*-$PHEP_{10}$	8.5×10^{-4}	90.0 ± 0.93	0.159 ± 0.006	−35.2
PCL_{50}-*b*-$PHEP_{15}$	1.4×10^{-3}	72.2 ± 0.32	0.113 ± 0.010	−35.2
PCL_{75}-*b*-$PHEP_{15}$	7.8×10^{-4}	110.0 ± 2.10	0.109 ± 0.022	−35.6
PCL_{100}-*b*-$PHEP_{18}$	6.1×10^{-4}	123.0 ± 0.44	0.080 ± 0.030	−36.4

It has been reported that many factors such as the polymer composition,[39] preparation method, and solvent of choice, etc.,[40] would influence the final morphology of the self-assembled aggregates from amphiphilic block copolymers. It is possible that with less hydrophilic PHEP component PCL_{50}-*b*-$PHEP_{15}$ (compared with PCL_{30}-*b*-$PHEP_{13}$) would intend to self-assemble into vesicular structure in aqueous solution. To further demonstrate this, we utilized the film rehydration method to prepare polymeric aggregates. Such a method has been used widely in the preparation of large liposome and polymersome.[41−43] In order to visualize the aggregates using confocal laser scanning microscopy, we labeled the aggregates with PKH26, a hydrophobic dye which shows a very low fluorescence in aqueous solution but an enhanced fluorescence in a hydrophobic environment.[44] The CLSM images of the two polymeric aggregates are shown in Figures 7C, D. The observed morphologies of PCL_{30}-*b*-$PHEP_{13}$ and PCL_{50}-*b*-$PHEP_{15}$ were obviously different. PCL_{30}-*b*-$PHEP_{13}$ aggregates were shown as solid red dots which could be considered as micellar particles. However, from Figure 7D, it can be clearly seen that red fluorescence of PKH26 was coming from the shell of the vesicular particles with a size of around a few micrometers, indicating the existence of a hydrophobic membrane and the formation of vesicles.

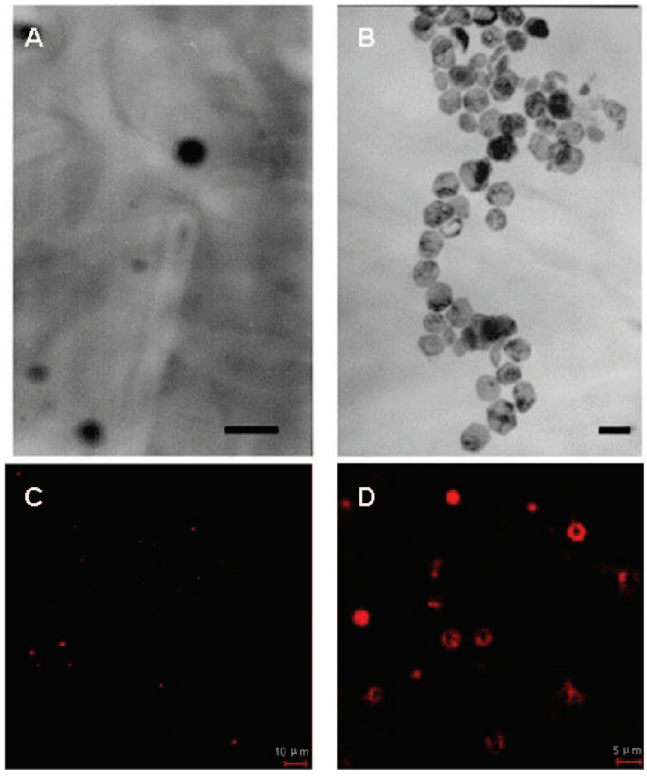

Figure 7. TEM images of polymeric aggregates of PCL-*b*-PHEP (A: PCL_{30}-*b*-$PHEP_{13}$; B: PCL_{50}-*b*-$PHEP_{15}$; scale bar = 100 nm) and confocal laser scanning micrographs of PCL-*b*-PHEP-based aggregates labeled with PKH26 (C: PCL_{30}-*b*-$PHEP_{13}$; D: PCL_{50}-*b*-$PHEP_{15}$).

In addition, using the pyrene solubilization technique that has been used widely for the determination of the CAC in block copolymer solutions,[45,46] it was observed that CAC value decreased from 4.6×10^{-3} to 6.1×10^{-4} g L^{-1} with the increase of PCL content (summarized in Table 3), which is reasonable since higher content of the hydrophobic segments will result in stronger interactions between hydrophobic chains, leading to a more stable structure and therefore to lower CAC value.[47]

Nanoparticles based on self-assembly of biocompatible amphiphilic block copolymers have been developed as drug delivery systems and showed great potential for therapeutic applications.[16,48−50] In the Supporting Information, it has been shown that cells cultured with PCL-*b*-PHEP remained viable when the concentration was up to 1 g L^{-1}. Our previous studies have also demonstrated the biocompatibility of polyphosphoester homopolymers[9] and block copolymers of PCL with polyphosphoesters.[8] For development of the drug delivery system, hydrophobic drug molecules have been loaded into the hydrophobic core of self-assembled micelles to increase drug solubility and to achieve passive accumulation in solid tumor tissues via the enhanced permeability and retention (EPR) effect,[17] while polymeric vesicles have shown a capacity for both hydrophobic and hydrophilic drug molecules, which are attractive due to the potential for simultaneous dual drug delivery.[18] With adjusting the composition, in this study, we proved that PCL-*b*-PHEP copolymer could self-assemble into aggregates with both micellar and vesicular conformations.

Conclusion

We have synthesized novel diblock copolymers PCL-*b*-PHEP based on biodegradable PCL and polyphosphoester bearing hydroxyl pendant groups. The structure of the diblock copolymers was well characterized by various methods. These block copolymers were amphiphilic and formed a micellar or vesicular structure in aqueous solution. The self-assembly behavior was demonstrated by the fluorescence probe method and further proved by DLS, TEM, and CLSM measurements, suggesting that the morphologies were actually dependent on the polymer compositions. No cytotoxicity of the polymers up to 1 mg/mL was observed by MTT assay. Further biomodification of the pendant hydroxyl groups is on progress in our laboratory now. We expect that the polymer would provide potential opportunities for pharmaceutical applications.

Acknowledgment. This work was supported by grants from National Natural Science Foundation of China (50733003, 20774089), Ministry of Sciences and Technology of the People's Republic of China (2006CB933300, 2009CB930301), and "Bairen" Program of Chinese Academy of Sciences.

Supporting Information Available: Plot of M_n vs $[GEP]_0/[PCL]_0$ feed ratio, ^{31}P NMR spectra of PCL_{30}-*b*-$PGEP_{13}$ and PCL_{30}-*b*-$PHEP_{13}$, excitation spectra of pyrene, and plot of the I_{338}/I_{335} ratio vs log *C*, and cytotoxicity study of block copolymer. This material is available free of charge via the Internet at http://pubs.acs.org.

References and Notes

(1) Heller, J.; Barr, J.; Ng, S. Y.; Abdellauoi, K. S.; Gurny, R. *Adv. Drug Delivery Rev.* **2002**, *54* (7), 1015–1039.
(2) Clapper, J. D.; Pearce, M. E.; Guymon, C. A.; Salem, A. K. *Biomacromolecules* **2008**, *9* (4), 1188–1194.
(3) Riva, R.; Schmeits, S.; Jerome, C.; Jerome, R.; Lecomte, P. *Macromolecules* **2007**, *40* (4), 796–803.
(4) Langer, R. *Acc. Chem. Res.* **2000**, *33* (2), 94–101.
(5) Athanasiou, K. A.; Agrawal, C. M.; Barber, F. A.; Burkhart, S. S. *Arthroscopy: J. Arthroscopic Relat. Surgery* **1998**, *14* (7), 726–737.
(6) Chew, S. Y.; Wen, J.; Yim, E. K. F.; Leong, K. W. *Biomacromolecules* **2005**, *6* (4), 2017–2024.
(7) Tian, D.; Dubois, P.; Grandfils, C.; Jerome, R. *Macromolecules* **1997**, *30* (3), 406–409.
(8) Wang, Y. C.; Tang, L. Y.; Sun, T. M.; Li, C. H.; Xiong, M. H.; Wang, J. *Biomacromolecules* **2008**, *9* (1), 388–395.
(9) Wang, J.; Mao, H. Q.; Leong, K. W. *J. Am. Chem. Soc.* **2001**, *123* (38), 9480–9481.
(10) Xu, X. Y.; Yee, W. C.; Hwang, P. Y. K.; Yu, H.; Wan, A. C. A.; Gao, S. J.; Boon, K. L.; Mao, H. Q.; Leong, K. W.; Wang, S. *Biomaterials* **2003**, *24* (13), 2405–2412.
(11) Parrish, B.; Breitenkamp, R. B.; Emrick, T. *J. Am. Chem. Soc.* **2005**, *127* (20), 7404–7410.
(12) Leemhuis, M.; van Nostrum, C. F.; Kruijtzer, J. A. W.; Zhong, Z. Y.; ten Breteler, M. R.; Dijkstra, P. J.; Feijen, J.; Hennink, W. E. *Macromolecules* **2006**, *39* (10), 3500–3508.
(13) Huang, S. W.; Wang, J.; Zhang, P. C.; Mao, H. Q.; Zhuo, R. X.; Leong, K. W. *Biomacromolecules* **2004**, *5* (2), 306–311.
(14) Du, J. Z.; Sun, T. M.; Weng, S. Q.; Chen, X. S.; Wang, J. *Biomacromolecules* **2007**, *8* (11), 3375–3381.
(15) Penczek, S.; Pretula, J. *Macromolecules* **1993**, *26* (9), 2228–2233.
(16) Kataoka, K.; Harada, A.; Nagasaki, Y. *Adv. Drug Delivery Rev.* **2001**, *47* (1), 113–131.
(17) Maeda, H.; Wu, J.; Sawa, T.; Matsumura, Y.; Hori, K. *J. Controlled Release* **2000**, *65* (1−2), 271–284.
(18) Ahmed, F. P., R. I.; Srinivas, G.; Brannan, A.; Bates, F.; Klein, M. L.; Minko, T.; Discher, D. E. *Mol. Pharmaceutics* **2006**, *3*, 340–350.
(19) Torchilin, V. P. *J. Controlled Release* **2001**, *73* (2−3), 137–172.
(20) Calvo, P.; Gouritin, B.; Brigger, I.; Lasmezas, C.; Deslys, J. P.; Williams, A.; Andreux, J. P.; Dormont, D.; Couvreur, P. *J. Neurosci. Methods* **2001**, *111* (2), 151–155.
(21) Edmundson, R. S. *Chem. Ind.* **1962**, 1828.
(22) Libiszowski, J.; Kaluzynski, K.; Penezek, S. *J. Polym. Sci., Polym. Chem. Ed.* **1978**, *16* (6), 1275–1283.
(23) Melvin, S.; Newman, M. R. *J. Am. Chem. Soc.* **1945**, *67* (9), 1621–1621.
(24) Kricheldorf, H. R.; Kreiser-Saunders, I.; Stricker, A. *Macromolecules* **2000**, *33* (3), 702–709.
(25) Save, M.; Schappacher, M.; Soum, A. *Macromol. Chem. Phys.* **2002**, *203* (5−6), 889–899.
(26) Biela, T.; Duda, A.; Penczek, S. *Macromol. Symp.* **2002**, *183*, 1–10.
(27) Lapienis, G.; Penczek, S. *Macromolecules* **1977**, *10*, 1301–1306.
(28) Lapienis, G.; Penczek, S. *J. Polym. Sci., Polym. Chem. Ed.* **1977**, *15*, 371–382.
(29) Pretula, J.; Penczek, S. *Makromol. Chem.* **1990**, *191*, 671–680.
(30) Penczek, S.; Pretula, J.; Kaluzynski, K. *J. Polym. Sci., Polym. Chem. Ed.* **2005**, *43* (3), 650–657.
(31) Biela, T.; Kubisa, P.; Penczek, S. *Makromol. Chem.* **1992**, *193*, 1147–1164.
(32) Xiao, C. S.; Wang, Y. C.; Du, J. Z.; Chen, X. S.; Wang, J. *Macromolecules* **2006**, *39* (20), 6825–6831.
(33) Wang, Y. C.; Shen, S. Y.; Wu, Q. P.; Chen, D. P.; Wang, J.; Steinhoff, G.; Ma, N. *Macromolecules* **2006**, *39* (26), 8992–8998.
(34) Wen, J.; Zhuo, R. X. *Polym. Int.* **1998**, *47* (4), 503–509.
(35) Detrembleur, C.; Mazza, M.; Lou, X.; Halleux, O.; Lecomte, P.; Mecerreyes, D.; Hedrick, J. L.; Jerome, R. *Macromolecules* **2000**, *33* (21), 7751–7760.
(36) Kowalski, A.; Duda, A.; Penczek, S. *Macromolecules* **1998**, *31* (7), 2114–2122.
(37) Amado, E.; Augsten, C.; Mader, K.; Blume, A.; Kressler, J. *Macromolecules* **2006**, *39* (26), 9486–9496.
(38) Sun, J.; Chen, X. S.; Deng, C.; Yu, H. J.; Xie, Z. G.; Jing, X. B. *Langmuir* **2007**, *23* (16), 8308–8315.
(39) Simone, E. A.; Dziubla, T. D.; Colon-Gonzalez, F.; Discher, D. E.; Muzykantov, V. R. *Biomacromolecules* **2007**, *8* (12), 3914–3921.
(40) Liu, X. Y.; Wu, J.; Kim, J. S.; Eisenberg, A. *Langmuir* **2006**, *22* (1), 419–424.
(41) Li, F.; Ketelaar, T.; Marcelis, A. T. M.; Leermakers, F. A. M.; Stuart, M. A. C.; Sudholter, E. J. R. *Macromolecules* **2007**, *40* (2), 329–333.
(42) Ghoroghchian, P. P.; Li, G. Z.; Levine, D. H.; Davis, K. P.; Bates, F. S.; Hammer, D. A.; Therien, M. J. *Macromolecules* **2006**, *39* (5), 1673–1675.
(43) Morishima, Y. *Angew. Chem., Int. Ed.* **2007**, *46* (9), 1370–1372.
(44) Dalhaimer, P.; Engler, A. J.; Parthasarathy, R.; Discher, D. E. *Biomacromolecules* **2004**, *5* (5), 1714–1719.
(45) Wilhelm, M.; Zhao, C. L.; Wang, Y. C.; Xu, R. L.; Winnik, M. A.; Mura, J. L.; Riess, G.; Croucher, M. D. *Macromolecules* **1991**, *24* (5), 1033–1040.
(46) Zhao, C. L.; Winnik, M. A.; Riess, G.; Croucher, M. D. *Langmuir* **1990**, *6* (2), 514–516.
(47) Du, J. Z.; Chen, D. P.; Wang, Y. C.; Xiao, C. S.; Lu, Y. J.; Wang, J.; Zhang, G. Z. *Biomacromolecules* **2006**, *7* (6), 1898–1903.
(48) Wang, F.; Bronich, T. K.; Kabanov, A. V.; Rauh, R. D.; Roovers, J. *Bioconjugate Chem.* **2005**, *16* (2), 397–405.
(49) Jeong, K. H.; Kim, Y. J. *Polymer—Korea* **2006**, *30* (6), 512–518.
(50) Kwon, G. S.; Forrest, M. L. *Drug Dev. Res.* **2006**, *67* (1), 15–22.

MA801043M